

Roger G Hipkin & Bernhard Steinberger  
Department of Geology & Geophysics  
University of Edinburgh, Edinburgh EH9 3JZ, United Kingdom

## SUMMARY

Gravity was measured at seven levels inside a submerged tower in Megget Water Reservoir, Scotland, in an experiment to test the inverse square law of gravitation over length scales from decimetres to tens of kilometres. The effects of Earth rotation, the global mass distribution, natural topography and man-made structures must be predicted at points outside the solid Earth, in order that that part of the measured attraction which is due to water in the reservoir can be separately identified. This attraction can be related to the Newtonian gravitational constant because, unlike natural rock masses, the density of water can be reliably predicted. This paper describes techniques aiming to determine all necessary corrections with a differential accuracy of  $5 \text{ nm.s}^{-2}$  over a 50 m vertical interval in order to exploit the  $10 \text{ nm.s}^{-2}$  accuracy available from LaCoste & Romberg gravity meters.

## INTRODUCTION

'Big G' experiments using water as the attracting test mass fall into two classes: those where the measurement point is fixed and a mass of water moves (for example the experiment in which a dry dock is filled, or the varying water level in a pump storage reservoir - see Edge & Oldham in this volume), and those, like the Megget Water experiment, where the attraction of a fixed mass of water is observed at different distances. The latter are inherently less tractable because the effect of all other masses, most particularly the topography, also changes as the observing position is moved and the contribution of the water must be isolated from them. The only redeeming feature of the second class of experiment is that the attraction of the water can amount to several milligals rather than only a few microgals, so that, in principle, greater accuracy in estimating the gravitational constant can be achieved. Practical realisation of this potential requires accurate and reliable computation of the attraction of all other masses.

## CORRECTIONS FOR THE GLOBAL GRAVITY FIELD

### Earth rotation and normal gravity

By first removing a reference gravity field, the main analysis need only deal with the anomalous gravity field, which is free of the effects of Earth rotation for measurements made at rest in a frame rotating with the Earth. Heiskanen & Moritz (1967) (H&M) give a closed formula on p 76 for 'normal gravity',  $\gamma$ , determined on the ellipsoid. This experiment evaluates it using the set of adopted parameters which define the Geodetic Reference System 1980. Comparison with recent observed values

implies that the scale of GRS80 normal gravity is uncertain by less than 4 parts in  $10^7$ . (Because this investigation is concerned with gravity differences, the accuracy of the GRS80 gravity datum, only about  $3900 \text{ nm.s}^{-2}$ , is not relevant to this experiment.)

Formulae used to determine the variation of normal gravity with height along the ellipsoidal normal need some caution because most are given and derived as series expansions and the accuracy required here is unusually large. H&M (p70) give a closed formula due to Brun's for the first derivative of normal gravity along the ellipsoidal normal. After some manipulation, it is

$$\frac{\partial \gamma}{\partial h} = \frac{-\gamma}{a(1-e^2)^{\frac{1}{2}}} (1-e^2 \sin^2 \phi)^{\frac{1}{2}} (2-e^2-e^4 \sin^2 \phi) - 2\omega^2 \quad (1)$$

Higher order derivatives generally involve approximations but a closed formula for them is derived here, using confocal ellipsoidal polar coordinates  $(u, \beta, \lambda)$  (H&M, sections 1.19 & 1.20). A curve following the ellipsoidal normal is obtained by varying  $u$ , essentially the semi-minor axis of the ellipsoids, and holding the other two coordinates fixed. Consequently, closed formulae for higher derivatives of normal gravity can be found by recasting Brun's formula (eq 1) in ellipsoidal polar coordinates and partially differentiating with respect to the minor axis. For example,

$$\frac{\partial^2 \gamma}{\partial h^2} = -\frac{1}{\gamma} \left( \frac{\partial \gamma}{\partial h} + 2\omega^2 \right) \frac{\partial \gamma}{\partial h} - \gamma \frac{\partial}{\partial h} \left[ \frac{1}{\gamma} \left( \frac{\partial \gamma}{\partial h} + 2\omega^2 \right) \right] \quad (2)$$

The first term is obtained from Brun's formula and the second is given after manipulation to and from ellipsoidal coordinates by the *exact* expression

$$\gamma \frac{\partial}{\partial h} \left[ \frac{1}{\gamma} \left( \frac{\partial \gamma}{\partial h} + 2\omega^2 \right) \right] = \frac{\gamma}{a^2(1-e^2)^2} \left( (2-e^2+e^4) - (7-e^2+e^4)\sin^2 \phi + 8e^4 \sin^4 \phi + (1-2e^2+2e^4)\sin^6 \phi \right) \quad (3)$$

Thus normal gravity can be calculated from a Taylor expansion about its value on the ellipsoid. For the location of the tower ( $\phi = 55^\circ.49508367$ ),

$$\gamma(h) = 9815494767. - 3084.80777h + 0.000722939h^2 - 0.0000000303h^3 \dots \text{nm.s}^{-2} \quad (4)$$

The highest observation point in the tower lies 336.00m above sea level, corresponding to an ellipsoidal height of about 390m. The quadratic term contributes  $26.6 \text{ nm.s}^{-2}$  to the gravity difference between the top and bottom of the tower but the cubic term is negligible at  $0.06 \text{ nm.s}^{-2}$ . However, this computation of the gravity



difference is a very significant  $87 \text{ nm.s}^{-2}$  smaller than the one given by the standard factor of  $3086 \text{ nm.s}^{-2}/\text{m}$  adopted by the Bureau Gravimetric International.

### The external effect of the anomalous gravity field

If the validity of the inverse square law is assumed, Laplace's equation holds. Predicting the external gravity field then only involves a surface integral of gravity anomalies; no assumptions are needed about the internal distribution of density.

However, integration is not trivial. Measurements of the anomalous gravity field are only available at discrete points on the Earth's topographic surface, and the integral can only be evaluated reliably if the anomalous field varies smoothly enough for valid interpolation between observations. The anomalous gravity field varies both because of lateral variations in subsurface rock density and because of the complex, non-ellipsoidal shape of the Earth's surface. Although the long wavelength components of the anomalous gravity field can be satisfactorily modelled as a finite spherical harmonic series, the effect of local topography generally predominates at short wavelengths. If great accuracy is required, this frustrates any attempt at direct integration for all but topographically benign regions: gravity observations cannot practically be made close enough together to recover short wavelength variations in ground height.

The difficulty can usually be circumvented by removing the calculated gravitational attraction of a model which represents the topographic geometry but assigns it a constant density. The difference between the observed 'free air' gravity anomalies and the attraction of the model topography are then related only to deviations from the assigned topographic density, together with lateral density variations at deeper levels. The short wavelength component of these 'complete Bouguer anomalies' is very greatly reduced compared with 'free air anomalies'. Consequently, the distance over which the anomalous gravity field can be adequately interpolated is increased and the maximum distance separating gravity observations become feasible.

The external effect of the anomalous gravity field was thus computed in three parts: first, the effect of long wavelength, global components; secondly, the effect of a local topographic model, and, thirdly, the contribution from differences between the global model and locally measured gravity anomalies, corrected for the attraction of local topography.

### Long wavelength gravity anomalies

The OSU86E spherical harmonic model of the anomalous gravity field (Rapp & Cruz, 1986) was used to calculate the global component of the anomalous gravity field. The model is complete to degree and order 360 and so, in principle, represents wavelengths longer than about 110 km.

The model field was calculated at 50m intervals along the ellipsoidal normal for heights between 0 and 700m above the ellipsoid. (The ellipsoidal height of the centre of the tower is about 364m.) This procedure required a high computational precision because each point requires the summation of more than 130000 terms. The anomalous gravity field was found to be

$$\Delta g_{\text{OSU86E}} = 31945.54 - 0.35926 h + 0.00000342 h^2 \text{ nm.s}^{-2}$$

The effect of the long wavelength components of the anomalous gravity field was thus a decrease of  $17.9 \text{ nm.s}^{-2}$  between the lowest and highest station in the tower.

## GEOMETRICAL MODELS OF LOCAL STRUCTURES

### Overview

Megget Water reservoir lies in a valley with the characteristic U-shaped cross-section of a glacial feature, having been deeply cut into Silurian greywackes during the Pleistocene. Nearby hills on its flanks rise 500 m above the valley floor and, although the draw-off tower in which the gravity measurements were made lies near the centre of the valley, analysis of the gravitational effect of topography requires special care. For all computations, a provisional value of  $6.673 \cdot 10^{-11} \text{ m}^3 \cdot \text{s}^{-2} \cdot \text{kg}^{-1}$  was adopted for the gravitational constant.

### Distant topography

The topographic model for distant topography was constructed from 1km square vertical prisms, whose height was estimated manually from 25' (7.6m) contour maps. These mean elevations were referred to a quadratic surface locally representing the curvature of the geoid. The gravitational attraction was computed from the full expression for a cuboid in an inner zone, with successive zones using the cylindrical sector and then the vertical line element approximations. A near zone, 8 km by 10 km, was excluded from the prism model which was extended to a distance of about 120 km before the incremental contribution differed by less than  $5 \text{ nm.s}^{-2}$  between the top and bottom of the tower.

### The contour integration program

The gravitational attraction of the remaining parts of the natural topography, together with models for the reservoir embankment, draw-off tower and water were determined using a development of the contour integration algorithm of Talwani & Ewing (1960). This involves analytic integration for the attraction of a horizontal polygonal lamina, combined with numerical integration over the vertical coordinate to find the bulk attraction. Extensive numerical comparisons were made with spheres, cylinders, cuboids, and parabolic domes (for whose gravitational attraction analytic formula exist), in order to find an adequate numerical integration routine and determine the necessary density of contour information.

Oldham (personal communication, 1988) reports that the results of our version of the contour integration program were insignificantly different from those obtained with an analytical surface integration over the triangular facets of a polyhedron defined by the same digitised contours.



## Intermediate topography

Within a region defined by the National Grid coordinates [ $315 \text{ km} < \text{Easting} < 325 \text{ km}$ ,  $617 \text{ km} < \text{Northing} < 625 \text{ km}$ ], but excluding an innermost rectangle  $750 \text{ m}$  by  $1025 \text{ m}$ , a topographic model was constructed by digitising at  $25 \text{ m}$  intervals along every  $100'$  ( $30.5 \text{ m}$ ) contour on Ordnance Survey maps. In the region later occupied by the western (most distant) end of the reservoir,  $25'$  ( $7.6 \text{ m}$ ) contours were digitised.

## Local topography

Before construction of the reservoir embankment was begun, control pillars were established on the adjacent hillsides and levelled in to Ordnance Survey bench marks. A photogrammetric survey was then carried out, from which  $2 \text{ m}$  contours were mapped at a scale of  $1:1250$ . This map, and all subsequent construction work, were referred to a local coordinate system parallel to the National Grid. The precise National Grid coordinates of the origin of the local system were no longer available but comparison of numerous landmarks common to both the local and Ordnance Survey maps determined them with a standard deviation of  $0.7 \text{ m}$ .

After the dam was complete but before the reservoir was full, a second photogrammetric survey was made and a second contour map produced. There were additional levelled control points on the dam, new access roads and water channels. From these two surveys, a model of the local topography was constructed by digitising at  $2.5 \text{ m}$  intervals along every  $2 \text{ m}$  contour on both maps. The natural topography was defined by the first photogrammetric survey, or the foundation of any subsequent earthworks or construction.

## The reservoir embankment

The reservoir embankment has a triangular cross-section which, at the centre of the valley, is about  $60 \text{ m}$  high and about  $160 \text{ m}$  wide. The embankment was constructed from compacted soil and gravel with a central vertical membrane of asphalt  $700 \text{ mm}$  thick. At the base of the membrane is a concrete inspection gallery running the length of the dam and set into grouted bedrock. From the control room on the down-stream face of the embankment, a second inspection and access gallery runs beneath the dam to the draw-off tower rising from the reservoir floor. The drinking water aquaduct and overflow spillway lie beneath the floor of this gallery.

The model for what is loosely called the dam includes all made ground: it includes superficial earthworks for embankments for new roads, water channels and landscaping, as well as the reservoir embankment itself. The model is essentially defined from engineering drawings, with additional control from the two photogrammetric surveys.

## The water draw-off tower

The concrete tower consists of two concentric circular cylindrical shells mounted on an octagonal base. The outside diameter is  $24 \text{ m}$  and the walls are  $700 \text{ mm}$  thick. Drinking water is drawn off on the up-stream side by ten  $1400 \text{ mm}$  diameter pipes,

two at each of five levels at 8 m intervals from the bottom of the reservoir. Where the water enters, the two cylindrical shells are connected by a solid concrete sector but, elsewhere, the cavity between them serves as an overflow spillway. There is a further inlet to the spillway at the base of the tower to provide a controlled volume of water for the river downstream. The surface level and volume flow of drinking water and compensation water are monitored continuously.

Gravity measurements were taken about 1.4 m west of the vertical axis of symmetry of the cylinders on concrete floors at seven levels in the tower. The axis of maximum symmetry was inaccessible. Although the tower geometry is superficially simple, an embedded lift shaft, pipes, stairs and galleries added to its complexity. Ultimately, more than 2 Mbyte of information was used to construct a model for the tower: digital horizontal cross-sections, determined with 1 mm precision from engineering drawings and randomly checked at the 10 mm level with confirmatory tape measurements, were prepared at 200 mm vertical intervals. To recover the detailed shapes of local horizontal structures, additional cross-sections were added at 20 mm intervals where necessary.

## Water

The model for water in the reservoir consisted of three parts. The most distant part was defined by 25' (7.6 m) contours from Ordnance Survey maps. The main contribution came from the area of the photogrammetric survey surrounding the tower. Finally, a small but not insignificant effect came from water in the pipework of the tower.

During the gravity observation programme, the water level was 1.72 m below the overflow datum at 334.00 m above sea level. For the most distant part of the model, defined by 25' contours, the effect of water filling the reservoir to 1025', 1050', 1075' and 1100' (335.28 m) was computed and the required effect of water at 332.28 m was found by linear, quadratic and cubic interpolation polynomials. The interpolation errors appeared to lie within  $5 \text{ nm.s}^{-2}$  at each site. The same interpolation procedure was used for the main contribution defined by the 2 m contour model, again with insignificant errors.

Water entering each of the drinking water inlet pipes is monitored continuously for temperature (to 0.1K), pH and gas content. It was apparent that the water was well mixed, with a top-to-bottom variation of temperature of less than 0.2K about a mean of  $7.2^{\circ}\text{C}$ . The atmospheric pressure was measured with precision surveying barometers with an accuracy of about 0.1bar. The density of water in the reservoir was thus determinable as  $(0.99988 \pm 0.00001) \text{ Mg.m}^{-3}$ .

## ANALYTIC CONTINUATION OF THE RESIDUAL BOUGUER ANOMALIES

In order to compute the variation with height of the residual Bouguer anomaly, all point gravity observations within the 126 km square [ $258 \text{ km} < \text{Easting} < 384 \text{ km}$ ,  $560 \text{ km} < \text{Northing} < 686 \text{ km}$ ] were extracted from an integrated gravity database (Hipkin & Hussain, 1982). Within this area, there are 8796 stations, mostly observed by the British Geological Survey or Edinburgh University. The mean station density of  $0.55 \text{ km}^{-2}$  was moderately uniform despite the difficult terrain because of helicopter and pedestrian surveys. All data were uniformly reduced, with an adopted



terrain density, constant throughout, of  $2.7 \text{ Mg.m}^{-3}$ . The reduction also adopted a value of  $6.673 \cdot 10^{-11} \text{ kg.m}^3.\text{s}^{-2}$  for the gravitational constant. Both figures are identical to the ones used to calculate the attraction of the topographic model, so that the combination is independent of these choices. Terrain corrections were completed to at least 22 km and usually to 64 km. Although duplicate and very closely spaced stations had been eliminated from the database, consistency between the two main surveys had previously been demonstrated at 100 - 400  $\text{nm.s}^{-2}$  level, compatible with their target accuracy of 500  $\text{nm.s}^{-2}$  (0.05 mgal).

The variation of the Bouguer anomaly with height in the tower was found as a by-product of a transformation algorithm described in Hipkin (1988). This Fast Fourier Transform routine was designed to transform point observations irregularly distributed over a topographically irregular surface to a regularly gridded representation on a plane. It was applied to the 126 km square of data with four options: first, the interpolation grid size was varied between 1 and 2 km; secondly, variable marginal tapering and optional linear detrending were applied before Fourier transformation; thirdly, the altitude of the horizontal plane was varied between 0 and 700 m above sea level, and, finally, the vertical gradient was determined either as a first derivative on the plane or by linear interpolation between values on two horizontal planes. These options generated slightly different estimates for the vertical gradient of the residual Bouguer anomaly: the mean and standard deviation of six estimating procedures were:

$$\Delta g(h) - \Delta g(0) = -(1.88 \pm 0.32) h \text{ nm.s}^{-2},$$

with a gradient range between -2.39 and -1.51  $\text{nm.s}^{-2}/\text{m}$ . The option likely to give the best result involved interpolation between planes separated by a 65 m vertical interval covering the tower measurements and used a detrended 2 km grid with a 10% marginal taper; it gave -1.85  $\text{nm.s}^{-2}/\text{m}$ .

This scatter reflects the fact that the data spacing was not quite close enough in the region around Megget Water to achieve the desired accuracy: one standard deviation in the Bouguer anomaly gradient generates 16  $\text{nm.s}^{-2}$  between the top and bottom of the tower.

### The effective topographic density

The constant density used in the topographic model was varied until its attraction calculated in the tower most closely approximated that of the combination of the Bouguer anomaly gradient of  $-(1.88 \pm 0.32) \text{ nm.s}^{-2}/\text{m}$  and the model using a density of  $2.7 \text{ Mg.m}^{-3}$ . This defined a locally effective mean topographic density of  $(2.7082 \pm 0.0014) \text{ Mg.m}^{-3}$ .

This figure can be compared with a direct gravimetric density determination in the area. All 196 point gravity observations in a 20 km square surrounding the tower were assumed to generate a Bouguer anomaly described by a second degree polynomial surface. The terrain density was then adjusted in a least squares minimisation of gravity residuals. This gave a local regression density of  $(2.7094 \pm 0.0030) \text{ Mg.m}^{-3}$ . (Note that both of these methods really estimate the product of density and the gravitational constant. The given value of density refers to the adopted value of the gravitational constant quoted above.)

The two methods of estimation are conceptually different: the second method



assumes that the topographic density is constant, whereas the first uses data which have not involved this assumption but merely approximate the result as a single effective density. It is however clear that the density really is unusually uniform: substituting the effective density into the topographic model calculation gives residuals against the original values with a standard deviation of only  $7.5 \text{ nm.s}^{-2}$  at the seven sites in the tower.

It was anticipated that the bedrock had uniform physical properties over a wide area. The Silurian greywacke formation, which some seismic models imply extends down to about 10 - 15 km, also extends over much of southern Scotland and Northern Ireland. Even on this scale, the density varies very little: Hipkin & Hussain (1982) used the regression density technique on 34 separate 10km squares and found an overall average of  $(2.728 \pm 0.045) \text{ Mg.m}^{-3}$  from 1688 gravity observations.

In the Megget Water valley, the conditions are particularly favourable: because of glaciation, the rockhead has been exposed from a depth of burial of at least 300 m in geologically recent times and so is virtually unweathered. Nevertheless, finding both estimates of the effective topographic density so similar and so well determined is particularly fortuitous and is crucial to the ultimate success of the experiment. It is almost always possible to find a 'pathological' density distribution which generates a measureable gravity field at some points and none at others. For this reason, any experiment based on predicting the external field from a finite set of point measurements needs recourse to a hypothesis that the field varies 'reasonably' between the observation points. Observable uniformity of the topographic density is *prima facie* evidence that it does.

## GRAVITY MEASUREMENTS

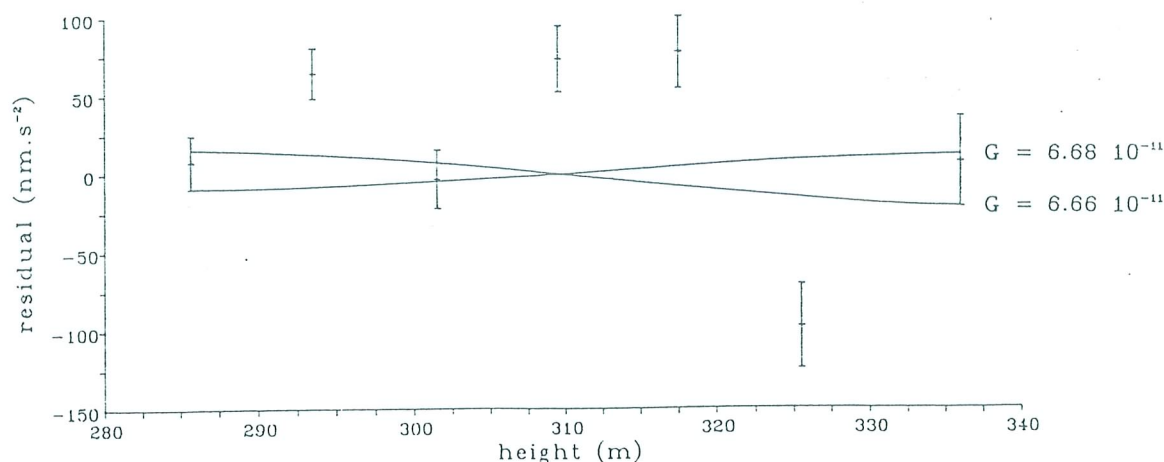
Gravity was measured at 7 sites within the tower and at 14 sites on the reservoir embankment. Analysis of the latter is incomplete and this paper gives a preliminary interpretation based on the tower measurements alone. The observations were made in a symmetrical triple looping sequence with the LaCoste & Romberg gravity meter G-275. This meter has been calibrated against the IGSN71 scale with a precision of 2 parts in 100000 (Hipkin et al 1988). The possibility of small gear train errors is currently being investigated by comparison with the gravity meters D-145 and D154, which have twin calibrated dials and electrostatic feedback. Given the gravity range of about 9 dial turns ( $90512 \text{ nm.s}^{-2}$ ) in the tower, the periodic screw errors are likely to be less than  $50 \text{ nm.s}^{-2}$ . Network adjustment using robust statistics with *a posteriori* weighting shows that the data have moderately good internal consistency, with a standard error of between 16 and  $29 \text{ nm.s}^{-2}$  at the tower sites. It is anticipated that additional observation sequences will halve this error.

## RESULTS AND DISCUSSION

Figure 1 shows residuals between observed and calculated gravity at each of the 7 tower sites, together with the effect of increasing or decreasing the gravitational constant from the adopted value of  $6.673 \cdot 10^{-11} \text{ m}^3.\text{s}^{-2}.\text{kg}^{-1}$ . Although adjustment would imply an insignificant correction to the laboratory value, the residuals are not only unacceptably larger than the observational errors, but also show systematic deviations in mid-elevations. The rate of variation with height in the upper half of



Figure 1: Gravity residuals in Megget Water Tower



the tower shows that the error must lie in computing the effect of the tower itself and, once any error is admitted, doubt is cast on the whole calculation. The experiment will only be convincing if the residuals have the magnitude expected from the observational data and are randomly scattered with respect to height. A probable source of the error in the tower model has now come to light: the present solution involves a uniform density found by regression, whereas the design specifications for steel re-enforcing show a progressively larger proportion of steel towards the base. The attraction of the tower will now be recomputed after modifying the effective density with height.

If a convincing balance of calculated and observed gravity can ultimately be achieved, it will imply that sources at distances ranging from a few centimetres in the tower to many tens of kilometres in the natural topography have all satisfied the inverse square law. The potential precision of better than 1 part in 1000 for the gravitational constant, combined with a demonstrable ability to determine the topographic and subsurface effects, makes the submerged tower form of experiment a very attractive approach for testing Newton's law of gravitation.

**Acknowledgements.** We wish to thank Lothian Regional Council's Department of Water & Drainage for their collaboration and assistance.

## REFERENCES

- Heiskanen, W & Moritz, H (1967). *Physical Geodesy*, Freeman, San Francisco.
- Hipkin, R G (1988) Bouguer anomalies and the geoid: a reassessment of Stokes' method, *Geoph. J.*, **92**, 53-66.
- Hipkin, R G & Hussain, A (1983) Regional gravity anomalies: I Northern Britain, *Rep. Inst. Geol. Sci.*, **82/10**, HMSO London.
- Hipkin, R. G., Lagios, E., Lyness, D & Jones, P. (1988) Reference gravity stations on the IGSN71 standard in Britain and Greece. *Geoph. J.*, **92**, 143-148.
- Rapp, R. H. & Cruz, J. Y. (1986) Spherical harmonic expansions of the Earth's gravitational potential to degree 360 using 30' mean anomalies, *Rep. Dept. geod. Sci. Surv., Ohio State Univ.*, **376**.
- Talwani, M. & Ewing, M. (1960) Rapid computation of the gravitational attraction of three-dimensional bodies of arbitrary shape, *Geophysics*, **25**, 203-225.